

Supplement Information

Biogeochemical model of CO₂ and CH₄ production in anoxic Arctic soil microcosms

Guoping Tang¹, Jianqiu Zheng², Xiaofeng Xu³, Ziming Yang¹, David E. Graham^{2,4}, Baohua Gu¹, Scott Painter^{1,4}, and Peter E. Thornton^{1,4}

¹Environmental Sciences Division, Oak Ridge National Laboratory, Oak Ridge TN, 37831 USA

²Biosciences Sciences Division, Oak Ridge National Laboratory, Oak Ridge TN, 37831 USA

³Biology Department, San Diego State University, San Diego, CA, 92182 USA

⁴Climate Change Science Institute, Oak Ridge National Laboratory, Oak Ridge TN, 37831 USA

Correspondence to: Guoping Tang (guopingtangva@gmail.com)

Table S1. Additional experimental parameter values summarized from (Herndon et al., 2015;Roy Chowdhury et al., 2015)

(TOTC = total organic carbon; WEOC = water extractable organic carbon; Acids = organic acids, f(pH) = pH factor).

Location	Horizon	Formate (mgC)	Acetate (mgC)	Propionate (mgC)	TOTC/d wt Soil	WEOC /TOTC	Acids/WE OC	f(pH)
Center	Oa	0.3162	1.7185	0.0445	38.35%	1.77%	21.69%	0.486
	Bgh	0.0198	0.3524	0.0213	13.78%	0.31%	10.23%	0.384
Ridge	Oe	0.0012	0.0046	0.0104	38.89%	0.54%	0.24%	0.601
	Bh	0.0270	0.3420	0.0399	14.65%	0.26%	12.46%	0.241
Trough	Oe	0.0016	0.0062	0.0140	20.55%	0.38%	0.66%	0.614
	Bh/ice	0.0204	0.2617	0.0104	7.99%	0.30%	14.53%	0.445

Table S2. Model parameter values for base scenario

Symbol	Value	Description
$f_{labile}f_{LabileDOC}$	0.0005	Initial fraction of LabileC in total organic carbon TOTC
$f_{somi1}f_{SOM1}$	0.01	Initial fraction of SOM1 in total organic carbon TOTC
$f_{somi2}f_{SOM2}$	0.02	Initial fraction of SOM2 in total organic carbon TOTC
$f_{somi3}f_{SOM3}$	0.1	Initial fraction of SOM3 in total organic carbon TOTC
$F_{FeRBferb}$	2×10^{-6}	Initial fraction of Fe reducers in total organic carbon TOTC
$F_{Mega}f_{mega}$	10^{-6}	Initial fraction of acetoclastic methanogens in total organic carbon TOTC
$F_{MegH}f_{megh}$	10^{-6}	Initial fraction of hydrogenotrophic methanogens in total organic carbon TOTC
f_{mega}	10^{-6}	Initial fraction of SOM4 in TOTC
$f_{Fe3}f_{Fe3}$	0.0025	Initial Fe(III) as a fraction of soil dry weight
$\phi_{labile}f_{Labile}$	0.4	Fraction of the original CLM-CN respiration factor goes through labile pool.

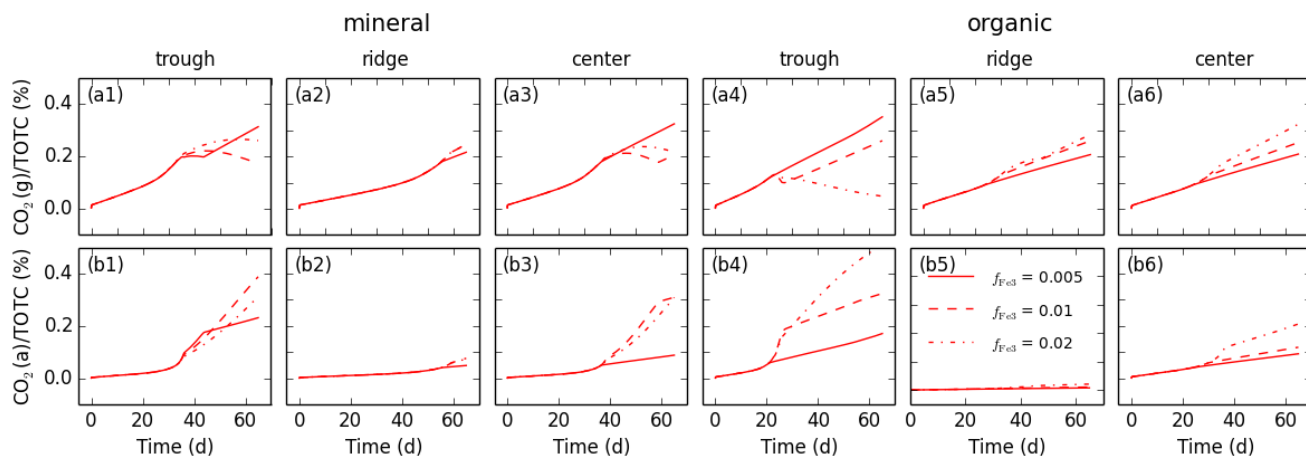


Figure S1: Calculated partition of CO_2 in gas and aqueous phases as a percentage of initial TOTC with different $f_{\text{Fe}3}$ values. The results correspond to Fig. 2 for temperature 8 °C. With increasing $f_{\text{Fe}3}$, the pH increases at the late times, as does the CO_2 solubility. [See Figure 2 caption for more information.](#)

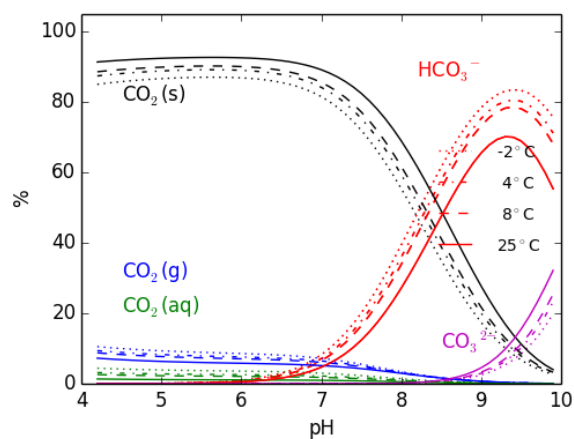


Figure S2: Adding 1 mmol $\text{Fe}(\text{OH})_{3a}$ into the numerical experiments shown in Fig. 3, the gas-phase fraction is decreased at low pH values [as the sorbed phase dominates.](#) [See Fig. 3 caption for more information.](#)

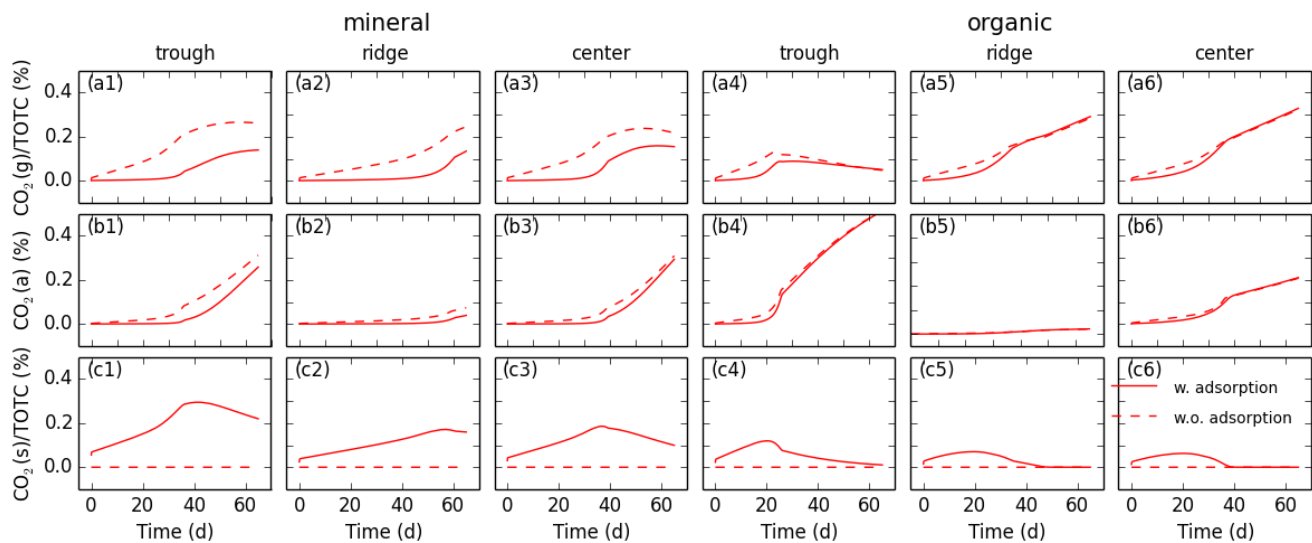


Figure S3: Impact of adsorption of CO_2 to ferric oxide surfaces on the distribution among gas, aqueous and solid phases. The gas phase concentration is predicted to be buffered by adsorption at the beginning. At late times, reduction and dissolution of $\text{Fe}(\text{OH})_{3a}$ sites may release CO_2 . See caption for Fig. 2 and Fig. S1 for more information.

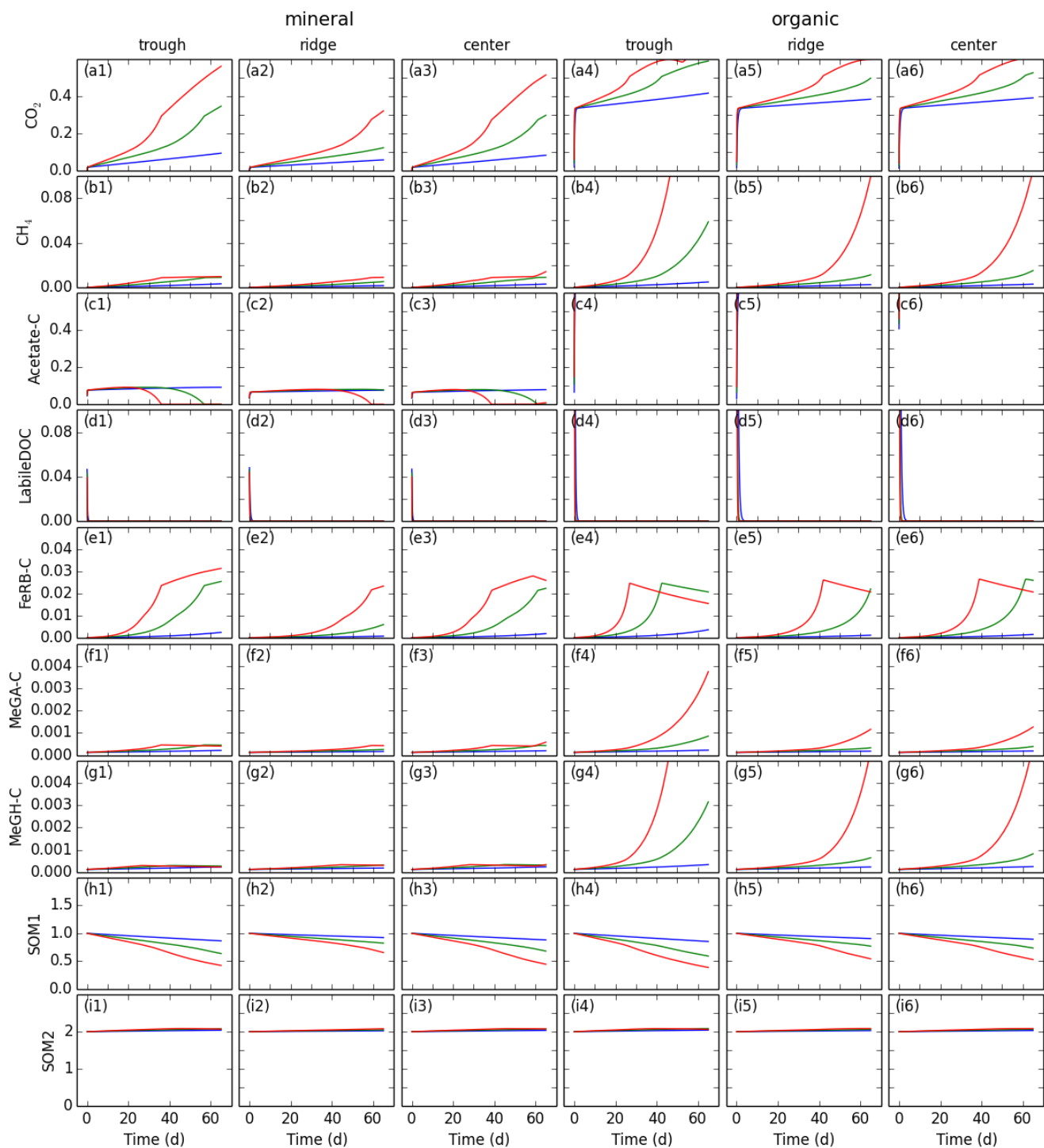


Figure S4: Partition of carbon among various organic pools. a, and b, and e are for total CO_2 distribution in the gas (head space), aqueous (water), and adsorbed (sorption to $\text{Fe}(\text{OH})_3$) and CH_4 in aqueous and gas phases. The recalcitrant pools (SOM3 and

SOM4) are the major fractions of soil organic carbon but have a slow turnover time relative to the experiment duration, therefore, not shown. See Fig.2 caption for more description about the model and experimental parameters.

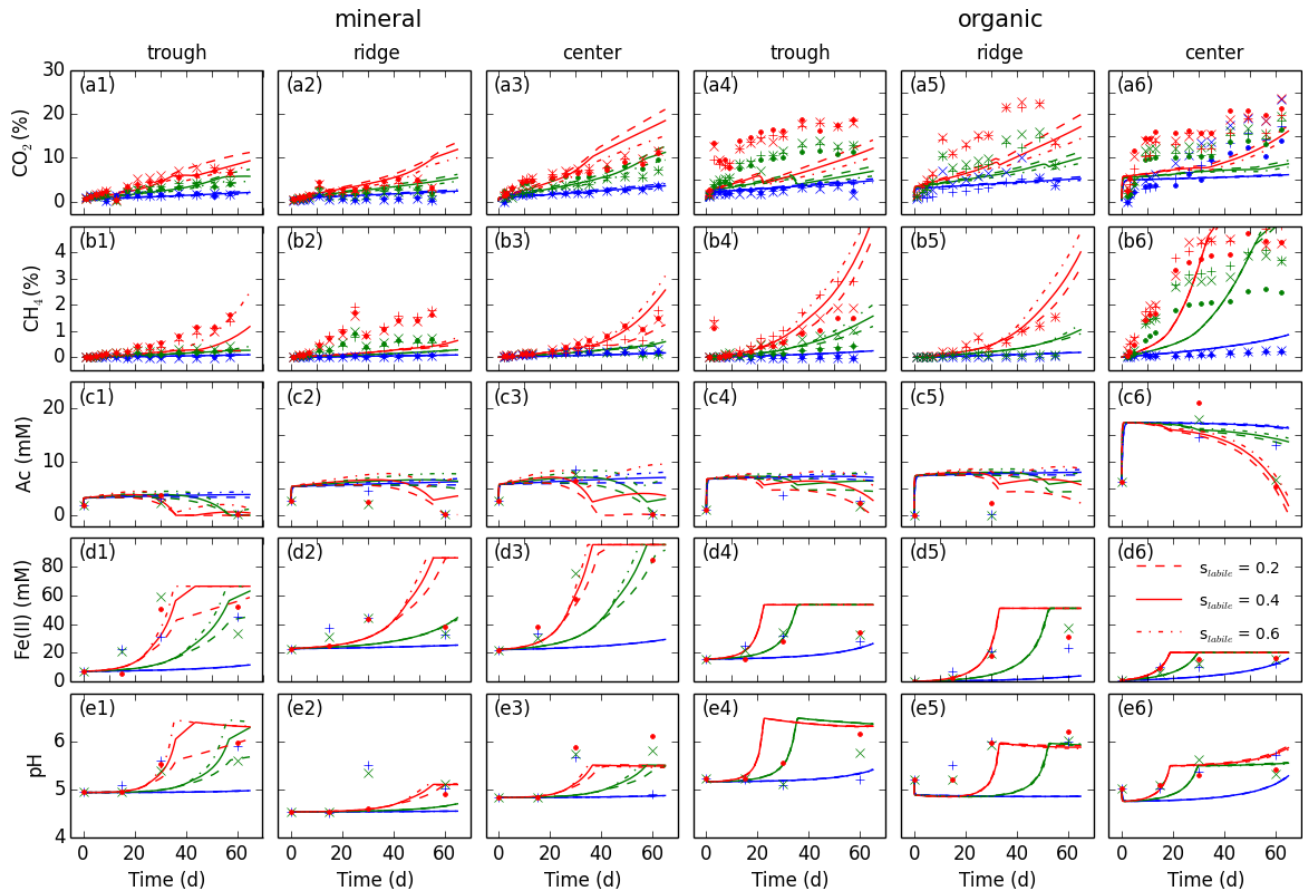


Figure S5: Impact of indirect respiration fraction (s_{labile}) on predictions: less direct respiration means more simple substrates for iron reduction and methanogenesis. See Fig.2 caption for more description about the model and experimental parameters.

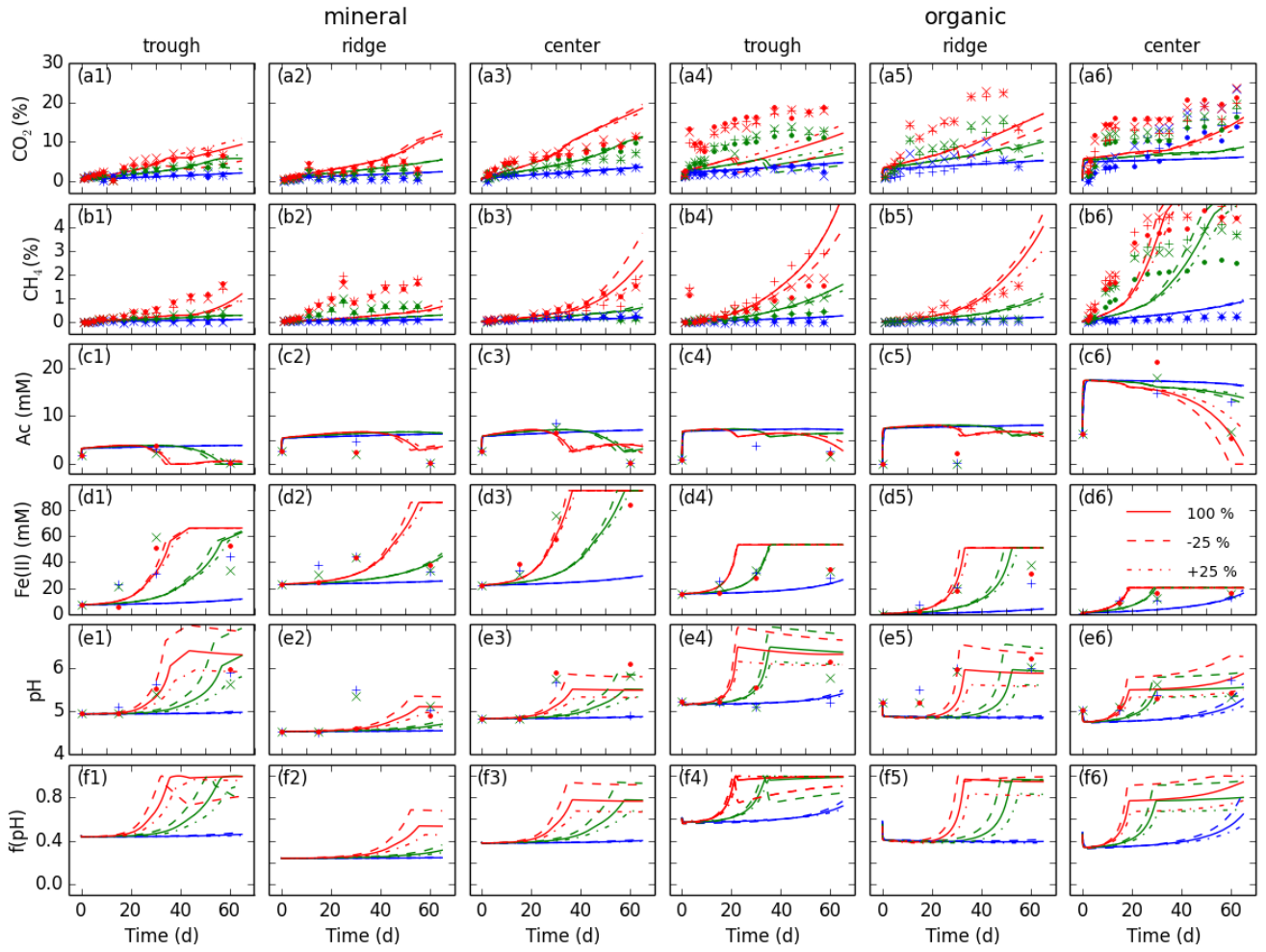


Figure S6: Impact of specified organic matter in WHAM on predictions: more organic matter means more pH buffer. See Fig.2 caption for more description about the model and experimental parameters.

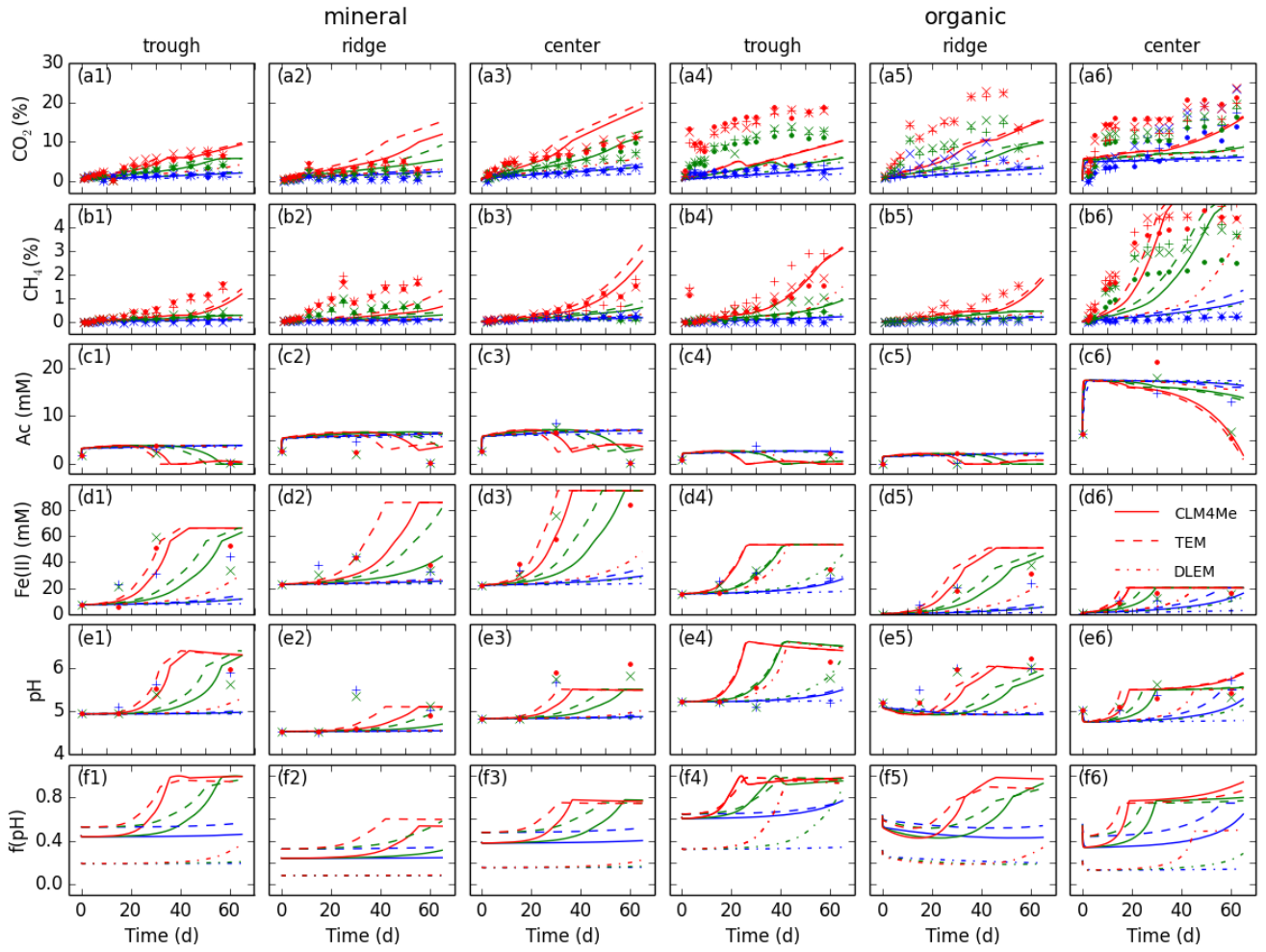


Figure S7: Comparison of the impact of different pH response functions (CLM4Me, TEM, and DLEM) on predictions. pH response function can be a substantial source of prediction uncertainty. See Fig.2 caption for more description about the model and experimental parameters.

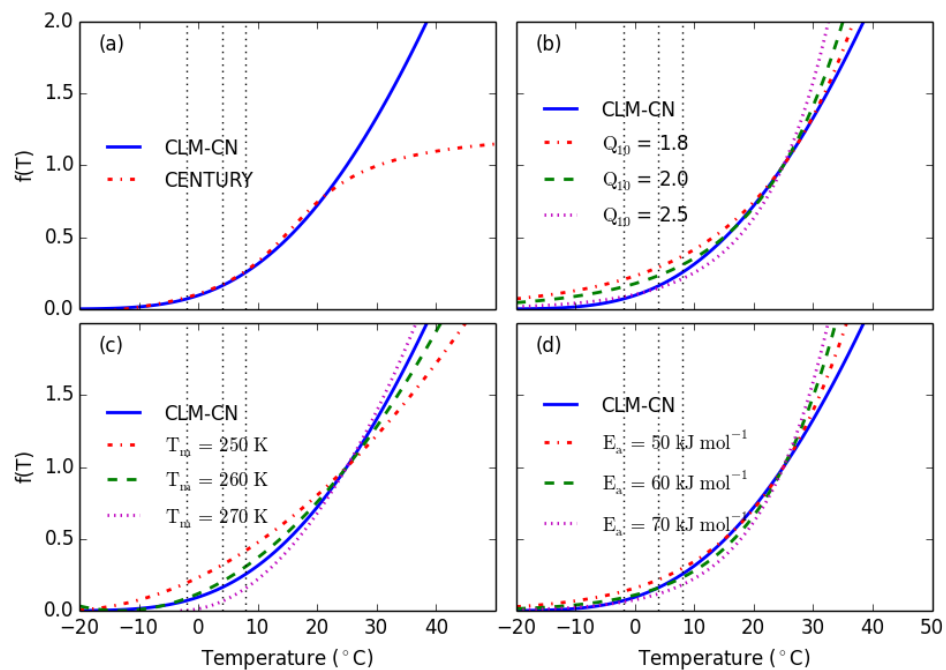


Figure S8: Fig. 7 with arithmetic vertical scale.

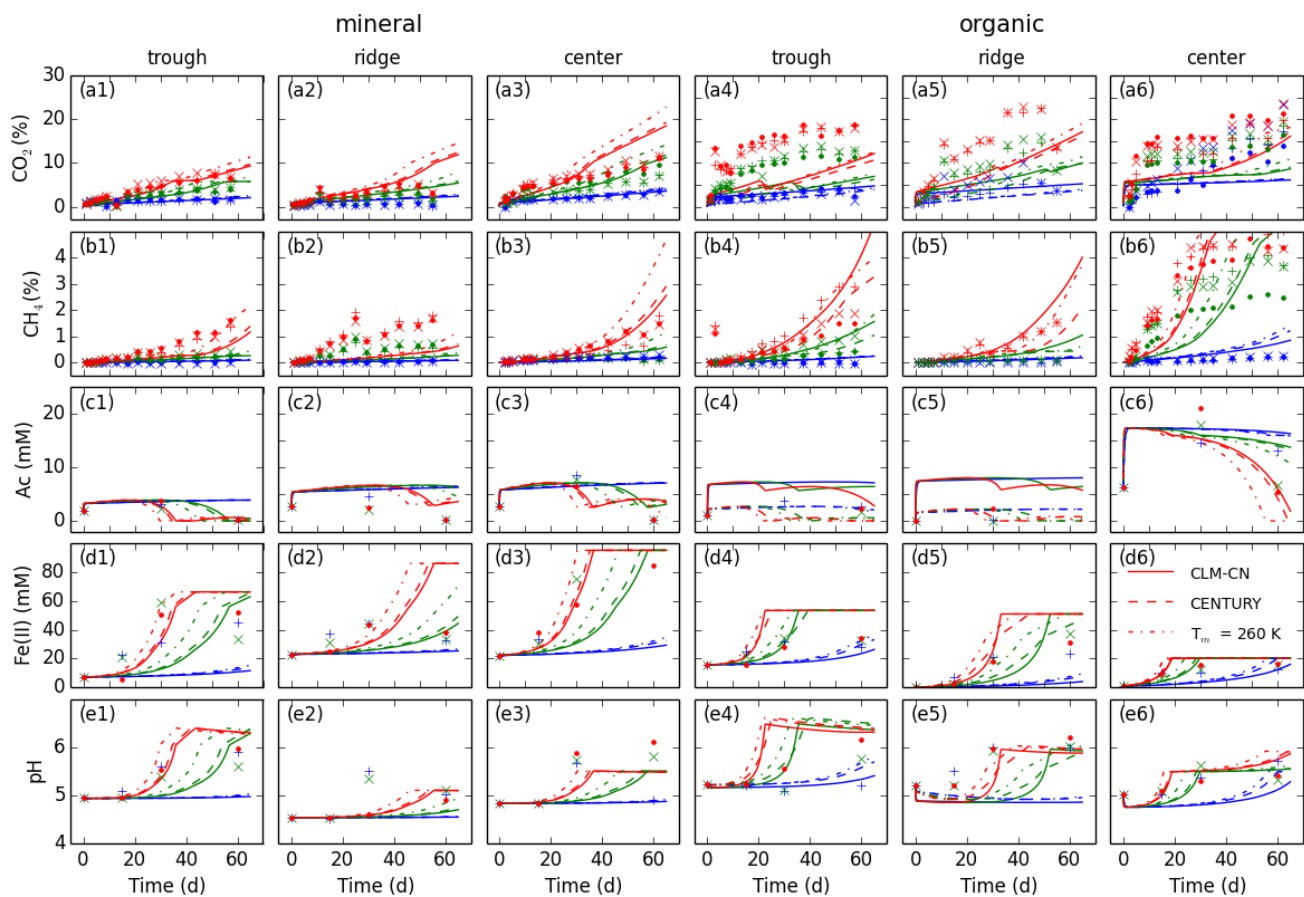


Figure S9: Comparison of impact of different temperature response functions (CLM-CN, CENTURY, Ratkowsky Equation with $T_m=260$) on predictions. Predictions are sensitive to temperature response function, which can introduce large prediction uncertainty. See Fig.2 caption for more description about the model and experimental parameters.

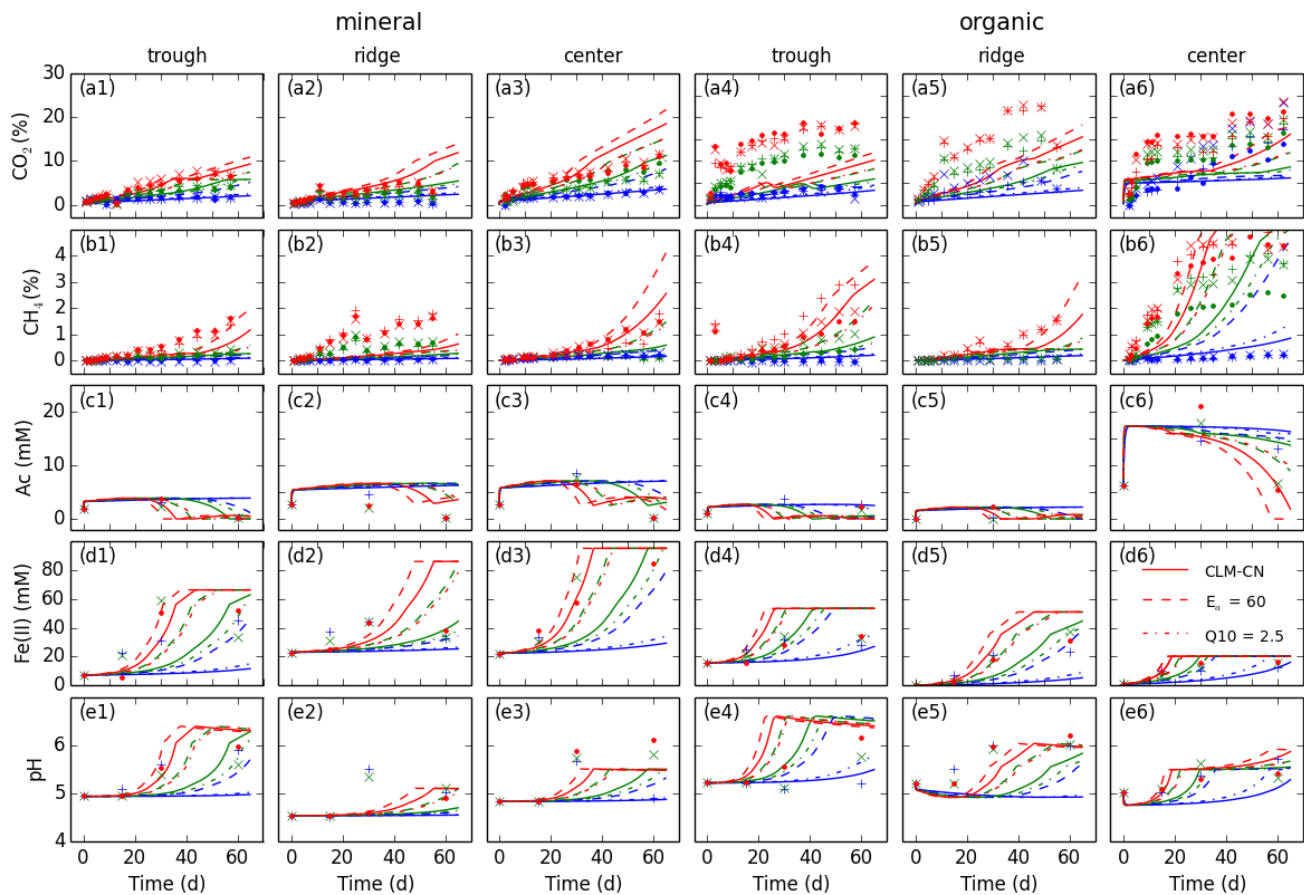


Figure S10: Comparison of impact of different temperature response functions (CLM-CN, Arrhenius equation (E_a), Q_{10} Equation) on predictions. Predictions are sensitive to temperature response function, which can introduce large prediction uncertainty. See Fig.2 caption for more description about the model and experimental parameters.

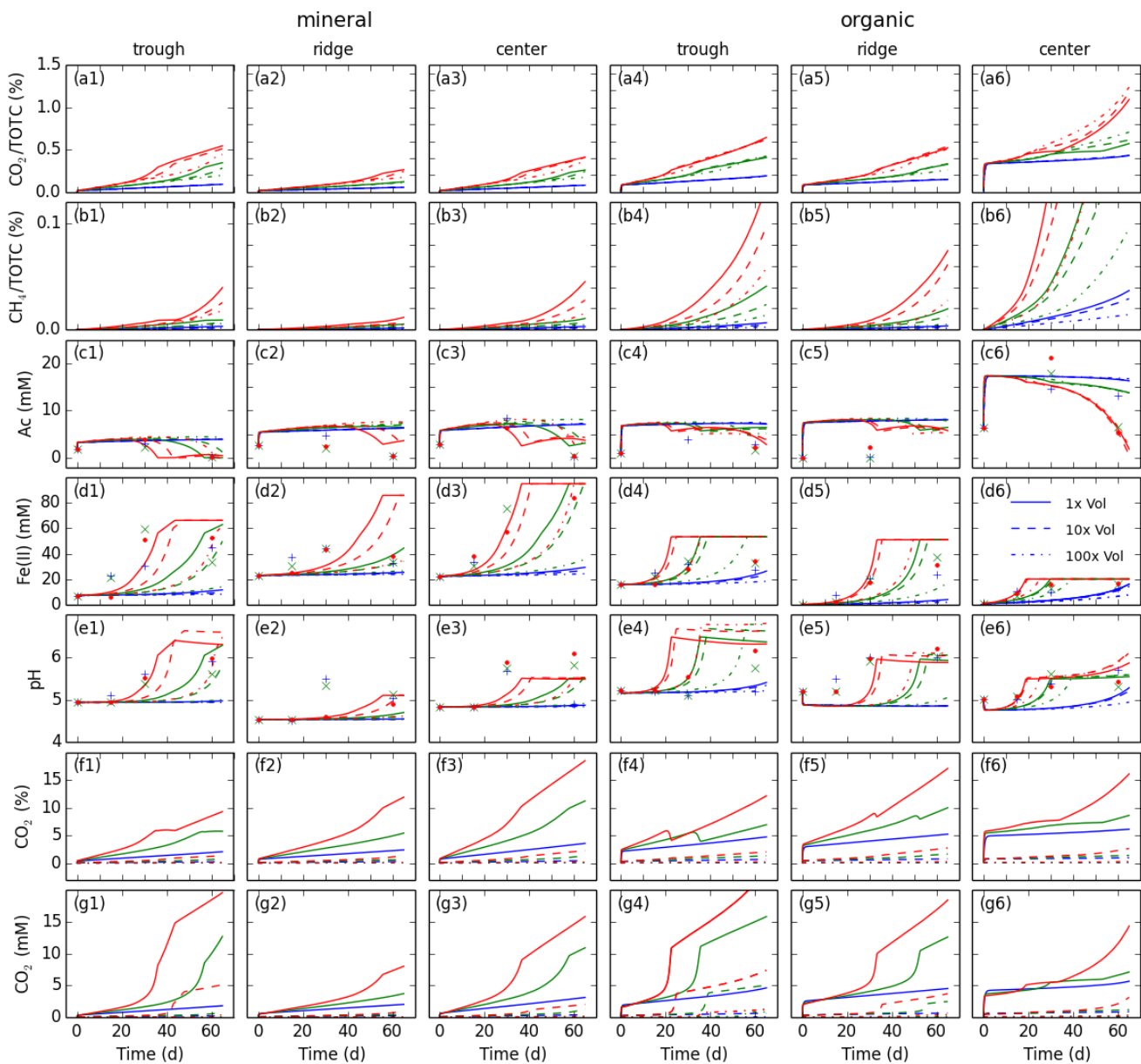


Figure S11: Impact of headspace volume on predictions: increase in headspace volume results in decrease in headspace (f1-6) and aqueous (g1-6) CO_2 concentration, slower pH increase and biogeochemical reaction rates, and generally less CO_2 and CH_4 production prediction. As an exception, predicted CO_2 production is increases with increasing headspace volume for the center organic soils. The impact is not linear as the underlying biogeochemical processes are nonlinear. TOTC = initial total organic carbon. Ac = organic acids as acetate. See Fig.2 caption for more description about the model and experimental parameters.

References

- Herndon, E. M., Mann, B. F., Chowdhury, T. R., Yang, Z., Wulfschleger, S. D., Graham, D., Liang, L., and Gu, B.: Pathways of anaerobic organic matter decomposition in tundra soils from Barrow, Alaska, *Journal of Geophysical Research: Biogeosciences*, n/a-n/a, 10.1002/2015JG003147, 2015.
- 5 Roy Chowdhury, T., Herndon, E. M., Phelps, T. J., Elias, D. A., Gu, B., Liang, L., Wulfschleger, S. D., and Graham, D. E.: Stoichiometry and temperature sensitivity of methanogenesis and CO₂ production from saturated polygonal tundra in Barrow, Alaska, *Global Change Biology*, 21, 722-737, 10.1111/gcb.12762, 2015.